Asociación Argentina
de Mecánica Computacional

Mecánica Computacional Vol XLII, pp. 627-636
A. Caggiano, G. Etse, P. Folino, M. Goldschmit, M. Pucheta, M. Storti (Eds.)
P. Folino, M. Ripani, S. Vrech (Issue eds.)
Buenos Aires, November 11-14, 2025

A NOVEL APPROACH FOR FRC SOFTENING LAW

Paula Folino[a,b], **Marianela Ripani**[a,c,e] **and Sonia Vrech**[d,e]

[a]*Universidad de Buenos Aires, Facultad de Ingeniería, Laboratorio de Métodos Numéricos en Ingeniería (LMNI). Buenos Aires, Argentina. pfolino@fi.uba.ar, mripani@fi.uba.ar*

[b]*Instituto de Tecnologías y Ciencias de la Ingeniería "Hilario Fernández Long" (INTECIN), UBA, CONICET. Buenos Aires, Argentina*

[c]*Universidad Nacional del Sur, Depto. de Ingeniería. Bahía Blanca, Buenos Aires, Argentina*

[d]*CEMNCI, Centro de Métodos Numéricos y Computacionales en Ingeniería. Universidad Nacional de Tucumán, Facultad de Ciencias Exactas e Ingeniería, Argentina. svrech@herrera.unt.edu.ar*

[e]*CONICET, Consejo Nacional de Investigaciones Científicas y Técnicas, Argentina*

Keywords: Fiber Reinforced Concrete, Post peak mechanical behavior, Bézier curves, Softening law.

Abstract. Post peak mechanical behavior of Fiber Reinforced Concrete (FRC) under tensile stress states depends not only on the fibers material, shape, content and slenderness but also, on the mechanical and physical properties of the cement paste. Being the improvement of ductility under tension, usually, the main purpose of adding fibers to the concrete composition, an accurate consideration of the resulting post peak behavior results a key parameter for an appropriate numerical simulation of the mechanical behavior of structural FRC elements. In this work, particularly focused on steel FRC, the suitability of cubic Bézier curves is analyzed, firstly, for determining Fracture Energy in mode I of FRC and then, for replacing the traditional exponential decay function usually used for characterizing the softening parameter in concrete constitutive formulations. The results show that the use of these parametric curves allows a flexible numerical approach that can be used for characterizing concretes with very different mechanical behaviors.

ISSN: 2591-3522 DOI: 10.70567/mc.v42.ocsid8529

1 INTRODUCTION

Concrete is a complex material characterized by a mechanical behavior governed, among other influence factors, by the stresses state. On the one hand, it presents a compressive strength much higher than its tensile one. On the other hand, while under uniaxial compression the material behaves in a way that can be classified as quasi-brittle, under uniaxial tension this behavior drastically turns to brittle while, on the contrary, under triaxial compression it almost turns to ductile with an increase in strength depending on the confinement level (van Mier, 1997).

The addition of fibers to the concrete, leading to Fiber Reinforced Concrete (FRC), has been proved to increase concrete ductility in tensile scenarios and to reduce crack widths by a bridge effect on open cracks (Banthia and Nandakumar, 2003; Barros et al., 2005; Buratti et al., 2011). However, regarding that the resulting composite material presents a mechanical behavior highly dependent on the FRC composition, cannot be properly characterized only by its strength properties. Any change in the fibers material, shape, slenderness or content, or in the cement matrix mechanical properties, lead to a different mechanical behavior. Therefore, Three Point Bending (TPB) or similar tests are necessary for obtaining the corresponding material fracture properties (See Model Code (MC1, 2012) and RILEM-TC-162-TDF (RIL, 2003)). Simplified methods for evaluating structural capacity consider the FRC Stress-Crack Opening relation as perfectly-plastic, linear o bilinear. However, considering the real FRC post peak behavior, those methods could not be enough accurate but conservative.

Bézier parametric curves are extensively used in the design of highways and railways, CAD systems, design of prototypes in many industrial applications (Martín et al., 2006; Habib and Sakaib, 2009; Sederberg, 2012), mesh design in FE environments (Menezes and Teodosiu, 2000), and also in the geometrical approximation of fibers in fiber reinforced composites (Kato and Ramm, 2009). Regarding failure and yielding surfaces, it can be mentioned the work by Vegter et al. (1995), who proposed a representation of the yield function using Bézier polynomials, interpolating mechanical tests results directly for the case of anisotropic metallic sheets, under a biaxial stresses state. In (Folino and Smilovich, 2015) a Bézier approximation was proposed for the interpolation between tensile and compressie meridians of yield surfaces in the deviatoric view. In this paper, it is explored the suitability of those parametric curves for modeling the post peak behavior of FRC.

2 BÉZIER CURVES

Bézier curves are defined by functions relating a set of given points, denoted as control points P_i, by blending functions in terms of a parameter $0 \leq t \leq 1$, and are represented by the following equation (Bézier, 2014; Piegl and Tiller, 1997)

$$B(t) = \sum_{i=0}^{n} \frac{n!}{i!\,(n-i)!}\,(1-t)^{n-i}\,t^i P_i \tag{1}$$

being n an integer number and $i = 0, 1, ..., n$.

In this work, cubic Bézier curves are applied, which are defined by four control points (See Fig.1), leading to a third-order polynomial in terms of parameter t. The broken line that can be formed connecting the control points, is called control polygon. Therefore, the coordinates of a curve $y = y_{(x)}$ can be represented by Eq. (2)

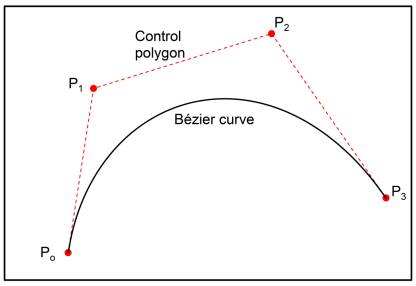

Figure 1: Typical cubic Bézier curve

$$\begin{cases} x(t) = (1-t)^3 x_o + 3(1-t)^2 t x_1 + 3(1-t) t^2 x_2 + t^3 x_3 \\ y(t) = (1-t)^3 y_o + 3(1-t)^2 t y_1 + 3(1-t) t^2 y_2 + t^3 y_3 \end{cases} \tag{2}$$

where x_i and y_i are the coordinates of each one of the four control points P_0, P_1, P_2 and P_3. Eq. (2) can be also written as detailed in Eq. (3), where coefficients a_x, b_x, c_x and d_x are functions of the x coordinates of the control points, while a_y, b_y, c_y and d_y are functions of the corresponding y coordinates.

$$\begin{cases} x(t) = a_x t^3 + b_x t^2 + c_x t + d_x \\ y(t) = a_y t^3 + b_y t^2 + c_y t + d_y \end{cases} \tag{3}$$

Bézier polynomials are characterized by the following properties: (1) The start point and end point of Bézier curve coincide with start point and end point of the control polygon, (2) The tangent vector of the curve at the start and end points coincides with the direction of the first and last edges of the control polygon, respectively, (3) The curve is inside the convex hull of the control polygon and (4) It is an approximation, not an interpolation, of the Control Points.

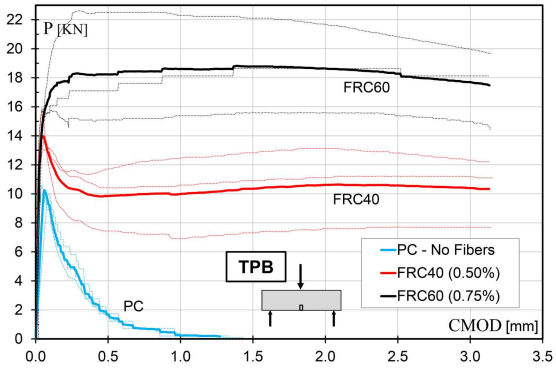

Figure 2: TPB tests: Load vs. CMOD

3 TPB TEST RESULTS REPRESENTED BY BÉZIER CURVES

In this Section, Bézier curves are applied for approximating the post peak non linear response of FRC in TPB tests, with two aims: (1) Convert the experimental data into a continuous curve, and (2) Obtain the fracture energy in mode I (G_f^I). For this purpose, the experimental results depicted in Fig. 2 are considered, corresponding to a normal strength concrete, plain (PC) and with two different contents of end-hooked steel macro-fibers, 40 kg/m^3 (FRC40) and 60 kg/m^3 (FRC60), rescpectively (For further details, see Folino et al. (2020)).

3.1 Load-CMOD TPB test curves

By applying Eq. (2) for approximating TPB tests post peak response, now coordinate x corresponds to the measured Crack mouth opening displacement ($CMOD$), and coordinate y, to the applied load (P) in the considered TPB test.

As previously explained, for creating a cubic Bézier approximation curve, it is necessary to define four control points. In this case, the first and last points (See Fig. 1), P_0 and P_3, respectively, correspond to experimental data. P_0 is defined as the limit of proportionality point, or in other words, the point where the non linear response starts, while P_3 is defined as the ultimate point of the experimental curve to be captured. For the intermediate points, the following expressions are proposed, based on the coordinates of points P_0 and P_3 and considering three parameters greater than zero, denoted as C_1, C_2 and C_3, to be calibrated for each data set, by an appropriate optimization procedure

$$\begin{aligned} P_1 \left\{ \; x_1 = C_1 \, x_0 \;\; ; \;\; y_1 = \frac{(y_0 - y_3)}{C_1} + \frac{y_3}{C_2} \right. \\ P_2 \left\{ \; x_2 = x_1 + \frac{(x_3 - x_1)}{5} \;\; ; \;\; y_2 = \frac{(y_0 - y_3)}{10 \, C_1} + \frac{y_3}{C_3} \right. \end{aligned} \tag{4}$$

Once the control points are defined, the curve is obtained based on Eq. (2) by adopting values for parameter t between 0 and 1. It is important to remark that t is itself a normalized coordinate along the length of the curve. In other words, for example t= 0.4 is located at the 40% of the curve length, starting from P_0.

Parameters C_1, C_2 and C_3 were calibrated in order to approximate the results in Fig. 2 and the resulting values are presented in Table 1. The obtained approximation curves are depicted in Fig. 3.

	Cubic Bézier				Other	
	C_1	C_2	C_3	R^2	R^2	
PC	4.80	0.97	1.00	0.996	0.994	(Exp.)
FRC40	4.00	2.05	0.86	0.988	0.945	(Polyn. 6th)
FRC60	1.50	0.88	0.88	0.921	0.929	(Polyn. 6th)

Table 1: Approximation curves for the TPB tests: Parameters and R-squared values for the Bézier curves and for other considered functions

In the case of PC, an exponential law was adopted to be compared with the Bézier curve. It is well known that an exponential decay function can appropriately represent the post peak behavior of plain concrete in a TPB test and therefore, there is no advantage to consider a Bézier function instead. On the contrary, when fibers are considered, an exponential law is not useful to approximate the corresponding complex non linear behavior. Therefore, 6^{th} degree polynomials were considered in the frame of this work in order to compare the corresponding results with the proposed Bézier approximation.

R-squared values R^2 obtained in each case are included in Table 1, where it can be seen that using a cubic Bézier approximation and considering only three parameters, the non linear behavior was captured with a good accuracy. The corresponding R^2 scores obtained for the

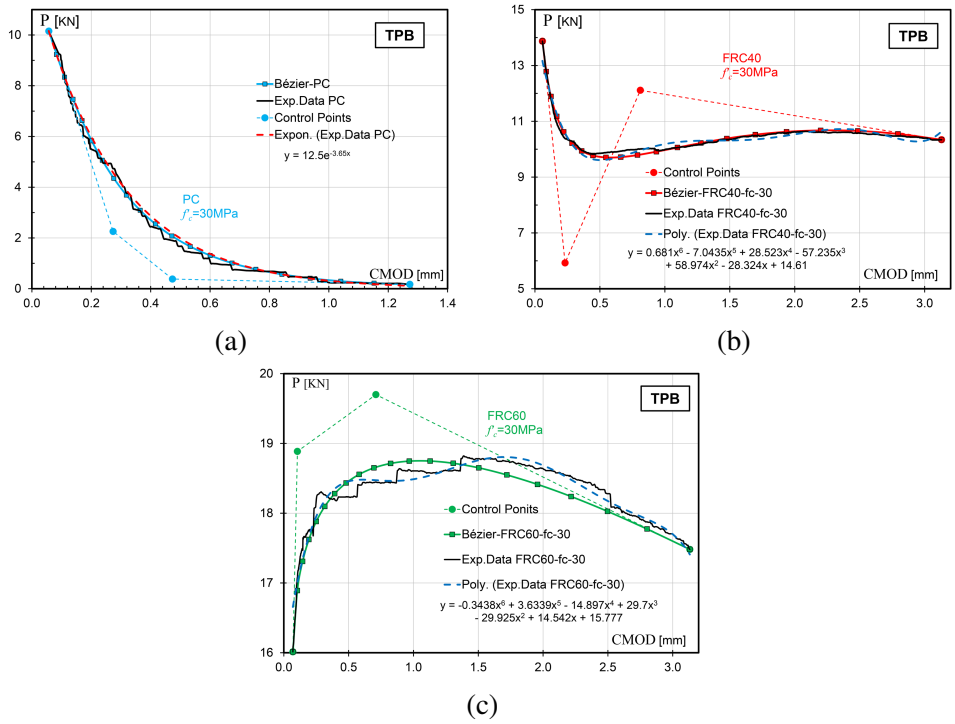

Figure 3: Bézier approximation curves for the nonlinear post peak response obtained in TPB tests (a) PC, (b) FRC40 and (c) FRC60

6^{th} degree polynomials are also included in Table 1 and it can be observed that in all cases the obtained results are very similar to those of Bézier approximations. In practice, a bilinear softening law is usually adopted for simulating the post peak response of FRC. However, the proposed three parameters Bézier approximation can improve numerical results, mainly in high complex constitutive modeling.

In regard to PC, from plots in Fig. 3(a) it can be concluded that the proposed cubic Bézier approximation can be used as an alternative of the exponential decay function regarding that similar R^2 values were obtained, demonstrating a good accuracy.

3.2 Fracture Energy G_f^I

Fracture energy in mode I, G_f^I, can be obtained from TPB tests on notched specimens under $CMOD$ control by calculating the area under the $P - CMOD$ curve and introducing a correction factor equal to 0.75 (Guinea et al., 1992; Michelini et al., 2023). Using a Bézier approximation and based on Eq. (3), the area under the Load-CMOD curve is determined as detailed in Eq. (5)

$$A = \int_0^1 y(t)x'(t)dt = a_x\left(\tfrac{1}{2}a_y + \tfrac{3}{5}b_y + \tfrac{3}{4}c_y + d_y\right) + b_x\left(\tfrac{2}{5}a_y + \tfrac{1}{2}b_y + \tfrac{2}{3}c_y + d_y\right) + \\ + c_x\left(\tfrac{1}{4}a_y + \tfrac{1}{3}b_y + \tfrac{1}{2}c_y + d_y\right) \tag{5}$$

As it can be observed, with the proposed formulation, G_f^I can be easily determined by a closed expression, in terms of the coordinates of the control points. For the analyzed cases, G_f^I values of 0.1067, 1.2777 and 2.2381 N/mm were obtained for PC, FRC40 and FRC60, respectively.

4 PROPOSED SOFTENING LAW FOR PLAIN AND FIBER REINFORCED CONCRETE

In this section, the obtained Bézier approximation is applied for transforming the exponential decay function of the softening, both for plain and FRC.

4.1 Typical softening law based on an exponential decay function

For the purpose of this Section, the Performance Dependent Model (PDM) (Folino and Etse, 2012) is used as a basis. This constitutive formulation, based on the three stress invariants, is applicable to predict the mechanical behavior of PC of different qualities.

Under continuous loading, when the peak load is reached at a material point, it means that the maximum strength surface is reached. At that moment, the softening law of the model is activated and plastic yield surfaces, defined in the Haigh Westergaard stresses space, are obtained by progressive contraction of the failure surface. These softening surfaces are associated to a softening parameter c which represents the decohesion as the ratio between the actual stress and the strength. It varies between a maximum value c=1 at peak strength, before activating the degradation or softening process in the material, and a minimum value $c = \sigma_{res}/\sigma_{max}$, being σ_{res} the residual strength and σ_{max}, the maximum one.

In the PDM, a fracture-energy based plastic softening law is adopted. The fracture energy G_f^I, defined as the energy necessary to create a crack of unit surface area in a plane parallel to the crack direction, A_t , is considered to be equal to the energy W dissipated during plastic softening in an equivalent elastoplastic continuum (See (Eq. 6)).

$$\begin{cases} dG_f^I \; A_t = \displaystyle\int_{A_t} \boldsymbol{\sigma}_t \; du_f \; dA & \text{(Discontinuous)} \\ \\ dW_f = \displaystyle\int_{V_t} \boldsymbol{\sigma}_t \; d\widetilde{\varepsilon}_f \; dV & \text{(Discontinuous)} \end{cases} \tag{6}$$

The rate of crack opening displacement $\dot{u}_f$ and the rate of the tensile fracture strains $\dot{\widetilde{\varepsilon}}_f$ uniformly distributed in the equivalent continuum are related by

$$\dot{u}_f = l_c \; \dot{\widetilde{\varepsilon}}_f \tag{7}$$

being l_c the characteristic length at the material level, acting as a gage length. In this case (mode I), the characteristic length l_c associated to a direct tensile test is represented as h_t. To extended this concept to a general mode II type of failure, the corresponding fracture energy G_f^{II} needs to be considered as well as the appropriate characteristic length. In case of PDM, the evolution of the softening parameter c is defined by an exponential decay function as

$$c = \exp\left(\frac{-\delta \; \kappa_s}{u_r}\right) \tag{8}$$

where κ_s is the fracture energy based softening measure, u_r the maximum crack opening displacement, and δ is a parameter defining the shape of the decay function. The evolution law of the fracture energy based softening measure κ_s is defined as

$$\dot{\kappa}_s = \dot{u}_f = l_c \; \dot{\widetilde{\varepsilon}}_f = l_c \; \| \langle \underline{\underline{\boldsymbol{m}}} \rangle \| \; \dot{\lambda} \tag{9}$$

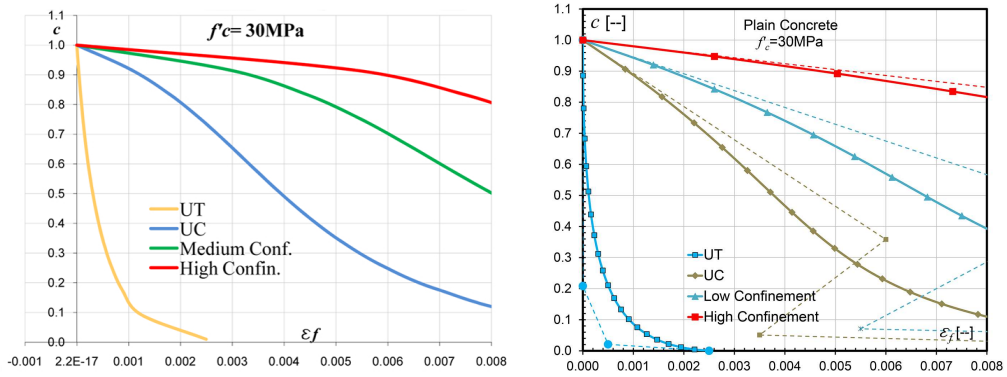

(a) (b)

Figure 4: Evolution of decohesion parameter c during softening process for different loading scenarios by applying (a) Exponential decay function and (b) Bézier polynomials

where the McCauley operator extracts only the tensile components of the gradient to the plastic potential $\underline{\underline{\boldsymbol{m}}}$ and λ is the plastic multiplier. The characteristic length l_c for mode II type of fracture is defined as

$$l_c = h_t \,/\, \omega_{(G_f^{II}/G_f^{I})} \tag{10}$$

where ω is an internal function of the PDM that estimates the ratio between the fracture energies in modes II and I (G_f^{II} and G_f^{I}) in terms of the acting confinement that is represented by the normalized first Haigh Westergaard stress coordinate $\overline{\xi}$ and depending on the concrete quality. In Fig. 4(a) it can be observed the PDM resulting evolution of the decohesion parameter c for a normal strength concrete.

4.2 Plain Concrete - Evolution of decohesion parameter c expressed by Bézier functions

In this Subsection, the evolution law based on the exponential decay function detailed in Eq. (8), is replaced by Bézier polynomials as

$$\begin{cases} \tilde{\varepsilon}_f(t) = a_{x(\kappa_s)}t^3 + b_{x(\kappa_s)}t^2 + c_{x(\kappa_s)}t + d_{x(\kappa_s)} \\ c(t) = a_{y(\kappa_s)}t^3 + b_{y(\kappa_s)}t^2 + c_{y(\kappa_s)}t + d_{y(\kappa_s)} \end{cases} \tag{11}$$

where now, coordinate x represents the tensile fracture strain and y, the decohesion parameter c.

The proposal involves the following hypotheses for the case of Uniaxial Tension (UT): (1) Coordinates of control point P_0 are $(0, 1)$; (2) Coordinates of control point P_3 are $(ur/lc, 0)$; (3) For the considered concrete type, apply the same parameters C_1, C_2 and C_3 in Eq. (4) estimated for the TPB test case for PC. Therefore, the evolution of c for the UT case is completely defined.

For increasing confinement levels: coordinate y of control point P3 is always equal zero, while coordinate x continuously evolves, considering that the characteristic length varies with confinement, causing a less localized failure type with higher confinement (Bažant and Pijaudier-Cabot, 1989). This value should be defined regarding the material quality and experimental data. Once defined the position of point P3, and considering that coordinates of P_0 are always $(0, 1)$, coordinates of points P1 and P2 are defined in terms of Point P3.

In Fig. 4(b) it can be observed the resulting evolution of the decohesion parameter c for a PC based on Bézier functions for different levels of confinement.

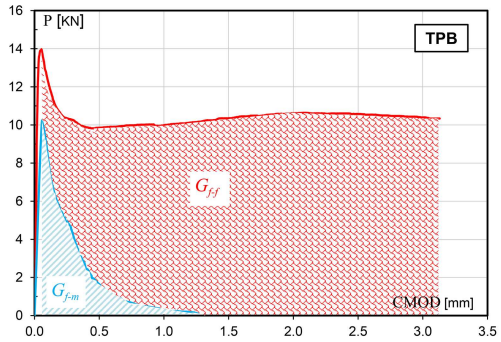

Figure 5: Fracture Energy for Fiber Reinforced Concrete in a TPB test

4.3 FRC - Evolution of decohesion parameter c expressed by Bézier functions

For PC, fracture energy increases with confinement level. On the contrary, in the case of FRC, fracture energy under tensile stress scenarios is not necessary smaller than that corresponding to uniaxial compression. This is due to the fact that fibers are activated when a crack tends to open. However, this contribution of the fibers is almost insignificant in the case of high confinements.

The total G_f^I obtaines from a TPB test, as it was previously described, can be decomposed in the contribution of plain concrete G_{f-m}^I and the contribution of fibers G_{f-f}^I as (See Fig.5)

$$G_f^I = G_{f-m}^I + G_{f-f}^I \tag{12}$$

The proposal herein is as follows:

- Modify the failure criterion by considering the FRC tensile strength
- Evaluate the total fracture energy of FRC G_f^I from TPB tests
- Evaluate the fracture energy of Plain Concrete G_{f-m}^I and obtain the corresponding contribution of the fibers G_{f-f}^I
- Determine for the FRC the evolution of c under Uniaxial Tension (UT): (1) Coordinates of control point P_0 are $(0, 1)$; (2) Coordinates of control point P_3 are calibrated considering the increase of fracture energy relative to the plain concrete case; (3) For the considered concrete type, apply the same parameters C_1, C_2 and C_3 in Eq. (4) estimated for the TPB test case for FRC.
- Consider the hypothesis that the contribution of G_{f-f}^I gradually disappears with increasing confinement. Therefore, the relation G_f^{II}/G_f^I gradually pass from the actual value under UT, to G_f^{II}/G_{f-m}^I for medium confinement levels. Evolution of parameter c can be seen in Fig. 6, where, in comparison with Fig. 4(b), it can be observed that only the UC is slightly affected by the contribution of fibers, while for medium and high confinement levels, almost no change is observed.

5 CONCLUSIONS

In the first part of this paper, cubic Bézier curves were proposed for approximating TPB test results of Fiber Reinforced Concrete. The results showed that a good accuracy can be obtained by appropriately calibrating three parameters. Once the resulting Bézier polynomial is obtained,

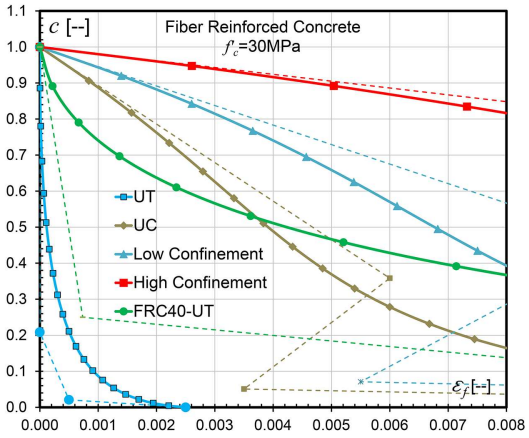

Figure 6: Evolution of decohesion parameter c for FRC40

it was demonstrated that Fracture Energy in mode I of the composite material can be obtained in a single step, in terms of the curve properties.

In the second part, the obtained Bézier approximation was applied for transforming the exponential decay function of the softening or decohesion parameter c, both for plain and for Fiber Reinforced concretes. The presented results demonstrated that a more flexible function is obtained particularly suitable for characterizing the post peak behavior of FRC.

The work presented herein is the first step of an ongoing research program. In the future, the proposal has to be implemented in the frame of a FE environment in order to obtain the structural response of FRC elements under different load scenarios. In particular, an extension for including the incidence of high temperatures on the mechanical behavior of FRC will be considered.

ACKNOWLEDGEMENTS

The authors gratefully acknowledge the financial support of the Universidad de Buenos Aires, Argentina through UBACyT 2023 No. 20020220100185BA Project and of the European Commission through the Marie Skłodowska-Curie Actions (MSCA) scheme under Grant Agreement ID: 101086440, through BEST (Bio-based Energy-efficient materials and Structures for Tomorrow) Project.

REFERENCES

RILEM-TC-162-TDF, test and design methods for steel fibre reinforced concrete: $\sigma - \epsilon$ design method - final recommendation. *Materials and Structures*, 36(262):560–567, 2003.

Model Code 2010 - Final Draft, volume 1-2. FIB Bulletin, 2012.

Banthia N. and Nandakumar N. Crack growth resistance of hybrid fiber reinforced cement composites. *Cement and Concrete Composites*, 25(1):3–9, 2003. http://doi.org/10.1016/S0958-9465(01)00043-9.

Barros J., Cunha V., Ribeiro A., and Antunes J. Post-cracking behaviour of steel fibre reinforced concrete. *Materials and Structures*, 38(1):47–56, 2005. http://doi.org/10.1007/BF02480574.

Bažant Z.P. and Pijaudier-Cabot G. Measurement of characteristic length of nonlocal continuum. *Journal of engineering mechanics*, 115(4):755–767, 1989. http://doi.org/10.1061/(ASCE)0733-9399(1989)115:4(755).

Bézier P. *The mathematical basis of the UNIURF CAD system*. Butterworth-Heinemann, 2014.

Buratti N., Mazzotti C., and Savoia M. Post-cracking behaviour of steel and macrosynthetic fibre-reinforced concretes. *Construction and Building Materials*, 25(5):2713–2722, 2011. http://doi.org/10.1016/j.conbuildmat.2010.12.022.

Folino P. and Etse G. Performance dependent model for normal and high strength concretes. *International Journal of Solids and Structures*, 49(5):701–719, 2012. http://doi.org/10.1016/j.ijsolstr.2011.11.020.

Folino P., Ripani M., Xargay H., and Rocca N. Comprehensive analysis of fiber reinforced concrete beams with conventional reinforcement. *Engineering Structures*, 202:109862, 2020. http://doi.org/10.1016/j.engstruct.2019.109862.

Folino P. and Smilovich D. Proposal of an interpolation function between the compressive and tensile meridians of failure and yielding concrete surfaces based on Bezier curves. In *PANACM 2015 - 1st Pan-American Congress on Computational Mechanics, in conjunction with the 11th Argentine Congress on Computational Mechanics, MECOM 2015*, pages 261–271. 2015.

Guinea G., Planas J., and Elices M. Measurement of the fracture energy using three-point bend tests: Part 1-influence of experimental procedures. *Materials and Structures*, 25(4):212–218, 1992. http://doi.org/10.1007/BF02473065.

Habib Z. and Sakaib M. G2 cubic transition between two circles with shape control. *Journal of Computational and Applied Mathematics*, 223:133–144, 2009. http://doi.org/10.1016/j.cam.2007.12.024.

Kato J. and Ramm E. Multiphase layout optimization for fiber reinforced composites applying a damage formulation. In *4th Colloquium on Textile Reinforced Structures (CTRS4), Anwendertagung, Dresden, Germany*, pages 337–354. 2009.

Martín L., Garriga C., Cremades L., and González M. Curvas bezier en el diseño de reflectores que satisfacen las necesidades de iluminación. In *X Congreso Internacional de Ingeniería de Proyectos, Valencia, España*, pages 779–785. 2006.

Menezes L. and Teodosiu C. Three-dimensional numerical simulation of the deep-drawing process using solid finite elements. *Journal of Materials Processing Technology*, 97:100–106, 2000. http://doi.org/10.1016/S0924-0136(99)00345-3.

Michelini E., Ferretti D., and Pizzati M. The influence of density on the fracture energy of aac: from experimental investigation to the calibration of a cohesive law. *Construction and Building Materials*, 400:132547, 2023. http://doi.org/10.1016/j.conbuildmat.2023.132547.

Piegl L. and Tiller W. *The NURBS book*. Springer-Verlag, Berlin, Germany, 1997. http://doi.org/10.1007/978-3-642-59223-2.

Sederberg T.W. Computer aided geometric design. *BYU, Computer Aided Geometric Design Course Notes*, 2012. Available from http://hdl.lib.byu.edu/1877/2822.

van Mier J. *Fracture Processes of Concrete*. CRC Press, Boca Raton, Florida, US, 1997.

Vegter H., Drent P., and Huetink J. A planar isotropic yield criterion based on mechanical testing at multi-axial stress states. In *Proceedings of the NUMIFORM 1995 Conference*, pages 345–350. 1995.